RP Current Trends In Applied Sciences (e-ISSN: 2583-7486)
Vol. 5, No. 2 (April – June 2026) pp. 104–109

RESEARCH PLATEAU PUBLISHERS

Cite this article: F. Mushahid, F. Firdaus, Physicochemical evaluation and preliminary biological performance of a Chitosan–fluorohydroxyapatite–Camellia *sinensis* ternary nanocomposite for bone tissue engineering, *RP Cur. Tr. Appl. Sci.* **5** (2026) 104–109.

Original Research Article

Physicochemical evaluation and preliminary biological performance of a Chitosan–fluorohydroxyapatite–Camellia *sinensis* ternary nanocomposite for bone tissue engineering

Fariha Mushahid, Farha Firdaus

Inorganic Chemistry Laboratory, Department of Chemistry, Aligarh Muslim University, Aligarh, India
*Corresponding author, E-mail: farihamushahid321@gmail.com

ARTICLE HISTORY
Received: 13 April 2026
Revised: 26 May 2026
Accepted: 27 May 2026
Published: 16 June 2026

KEYWORDS
Bone tissue engineering; Fluorohydroxyapatite; Chitosan; nanocomposite; Camellia sinensis; Biomineralization.

ABSTRACT
Bone tissue engineering seeks biomaterials that replicate the mineral composition of bone while providing surface features that support biological interactions. In this study, a CS-FHA-CMS ternary nanocomposite was developed and evaluated with emphasis on physicochemical properties and preliminary biological performance. The nanocomposite was synthesised using a wet chemical method and characterised by Fourier transform infrared spectroscopy, X-ray diffraction, and scanning electron microscopy. FTIR analysis confirmed the presence of apatite, polymeric, and polyphenol-associated functional groups, while XRD results demonstrated retention of the FHA crystalline phase with controlled crystallinity. SEM observations revealed a rough, porous surface morphology that is favourable for bone tissue integration. In vitro bioactivity assessed in simulated body fluid showed apatite layer formation, indicating osteoconductive behaviour. Short-term cytocompatibility, evaluated by the MTT assay, demonstrated high cell viability, confirming the non-cytotoxic nature of the composite. Overall, the findings highlight the potential of the CS–FHA–CMS nanocomposite for bone tissue engineering applications.

1. Introduction

Bone tissue engineering aims to develop biomaterials capable of supporting bone regeneration by mimicking the composition and microenvironment of native bone. An ideal scaffold should be biocompatible, bioactive, and possess surface characteristics that promote cell attachment, mineralisation, and tissue integration, while maintaining adequate structural stability. Achieving this balance remains a key challenge in the design of bone-regenerative materials [1].

Hydroxyapatite-based ceramics are widely employed in bone tissue engineering due to their close chemical similarity to the mineral phase of bone and their inherent osteoconductivity [2]. However, stoichiometric hydroxyapatite often exhibits limited biological stimulation and slow remodelling. Ionic substitution within the apatite lattice, such as fluorine incorporation, has been shown to improve crystallinity, stability, and biological performance by modulating surface chemistry and ion release behaviour [3]. FHA, therefore, represents a promising bioactive phase for bone scaffold development [4].

To further enhance biological functionality, hydroxyapatite is frequently combined with natural polymers. CS has attracted considerable interest due to its biocompatibility, biodegradability, and favourable interactions with inorganic phases, providing a supportive matrix that enhances processability and surface functionality [5]. In addition, the incorporation of polyphenol-rich herbal extracts has emerged as an effective strategy for introducing antioxidant and biofunctional cues into scaffold systems [6]. CMS (green tea) is rich in catechins and polyphenols and is expected to promote calcium phosphate deposition and influence early osteogenic cellular responses, as seen in previous studies [7]. In this context, the present study reports the development and preliminary evaluation of a CS-FHA–CMS ternary nanocomposite. The work focuses on physicochemical characterisation and limited biological validation to establish structure–bioactivity relationships and assess the material's potential for bone tissue engineering applications.

2. Materials and methods

2.1 Materials

Chitosan (medium molecular weight, degree of deacetylation ≥ 80%) was used as the polymeric matrix. Calcium nitrate tetrahydrate, diammonium hydrogen phosphate, and ammonium fluoride were employed as precursor materials for the synthesis of FHA. *CMS* extract was used as the bioactive herbal component. All chemicals were of analytical grade and used as received without further purification. Deionised water was used throughout the experimental procedures.

2.2 Synthesis of fluorohydroxyapatite

FHA was synthesised via a wet chemical precipitation method following previously reported procedures with minor

modifications [8]. Aqueous solutions of calcium and phosphate precursors were prepared separately, maintaining a Ca/P molar ratio of 1.67. The phosphate solution was added dropwise to the calcium solution under continuous stirring, and the pH was adjusted to ~10 using ammonia solution. Fluoride ions were introduced by the controlled addition of ammonium fluoride during the reaction. The reaction mixture was maintained at ~60–70 °C under constant stirring for 2–3 h, followed by ageing for 24 h at room temperature. The precipitate was then filtered, washed with deionised water to remove impurities, and dried at ~80 °C for 12 h to obtain FHA powder.

2.3 Preparation of CMS extract

The *CMS* extract was prepared using an aqueous extraction method as reported in the literature [9]. Dried green tea leaves were washed, air-dried, and finely ground. A known quantity of powdered leaves (e.g., 5 g) was mixed with distilled water (100 mL) and heated at ~60–80 °C for 30–60 min under continuous stirring. The mixture was then cooled and filtered to remove solid residues. The obtained filtrate was stored at 4 °C for further use.

2.4 Fabrication of CS-FHA-CMS nanocomposite

The ternary nanocomposite was fabricated by dispersing the synthesised FHA in a CS solution under continuous stirring. The *CMS* extract was then added gradually to the CS–FHA mixture to ensure uniform distribution of bioactive constituents. The resulting suspension was stirred until a homogeneous composite was obtained, followed by casting and drying to form the CS–FHA–*CMS* nanocomposite.

2.5 Physicochemical characterisation

FTIR spectroscopy was employed to identify functional groups and confirm interactions among the composite constituents. XRD analysis was performed to determine the phase composition and crystallinity of the nanocomposite. Surface morphology and microstructural features were examined using SEM.

2.6 In-vitro bioactivity assessment in simulated body fluid

In vitro bioactivity was evaluated by immersing the nanocomposite samples in SBF prepared according to established protocols [10]. The samples were incubated at physiological temperature for 15 days. After immersion, the samples were rinsed, dried, and analysed by SEM to observe apatite layer formation on the surface.

2.7 Cytocompatibility assessment (MTT Assay)

The cytocompatibility of the nanocomposite was evaluated using the MTT assay on MG-63 cells following standard protocols. Cells were cultured under appropriate conditions and exposed to different concentrations of the nanocomposite for 24 h. After incubation, MTT reagent was added, and the formed formazan crystals were dissolved and quantified spectrophotometrically. Untreated cells served as the control, and cell viability was expressed as a percentage relative to the control group.

2.8 ALP activity assay

Alkaline phosphatase (ALP) activity was evaluated using MG-63 cells to assess early osteogenic response. Cells were cultured and exposed to the nanocomposite for 1, 3, 7, and 10 days. ALP activity was quantified using a standard colorimetric assay and expressed relative to the control.

3. Results and discussion

3.1 FTIR analysis

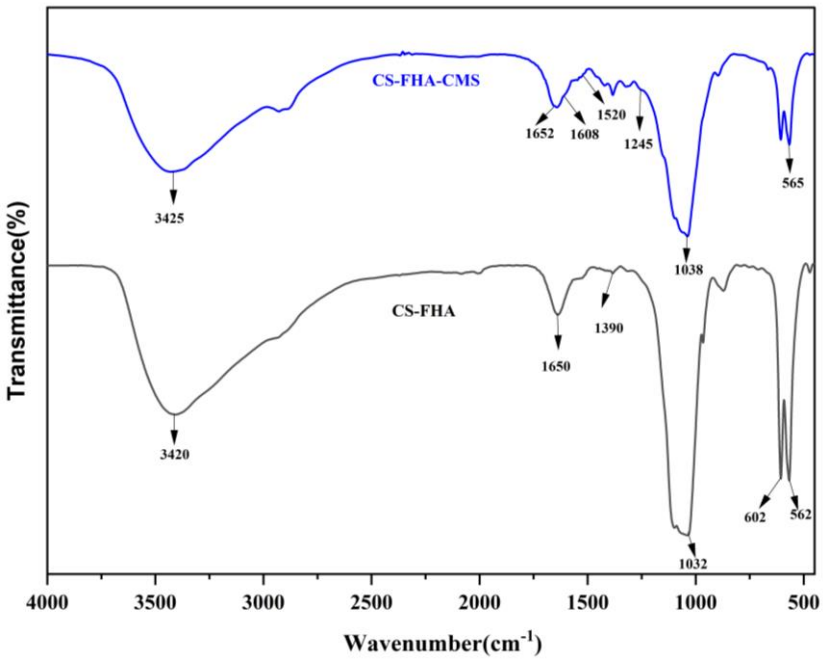

Figure 1: FTIR spectra of CS–FHA and CS–FHA–CMS nanocomposites.

The FTIR spectra of CS–FHA and CS–FHA–CMS are shown in Fig. 1. Both samples display a broad band at 3420–3425 cm^{-1} corresponding to overlapping O–H and N–H stretching vibrations of chitosan [11]. A slight broadening in the CMS-containing composite suggests modification of the hydrogen-bonding environment due to the presence of polyphenolic hydroxyl groups [12]. The amide I band is observed at 1650–1652 cm^{-1}, indicating that the chitosan backbone remains structurally preserved after composite formation [13]. In CS–FHA–CMS, additional bands at 1608 cm^{-1} and 1520 cm^{-1} are assigned to aromatic C=C skeletal vibrations associated with polyphenolic structures and the band at 1245 cm^{-1} corresponds to phenolic C–O stretching vibrations [14]. The characteristic PO_4^{3-} stretching band appears at 1032–1038 cm^{-1}, along with bending modes at 602–562 cm^{-1}, confirming retention of the FHA phase [15]. The slight shift in the phosphate band may indicate weak interfacial interactions between phenolic groups and surface calcium sites, without altering the apatite framework.

3.2 XRD analysis

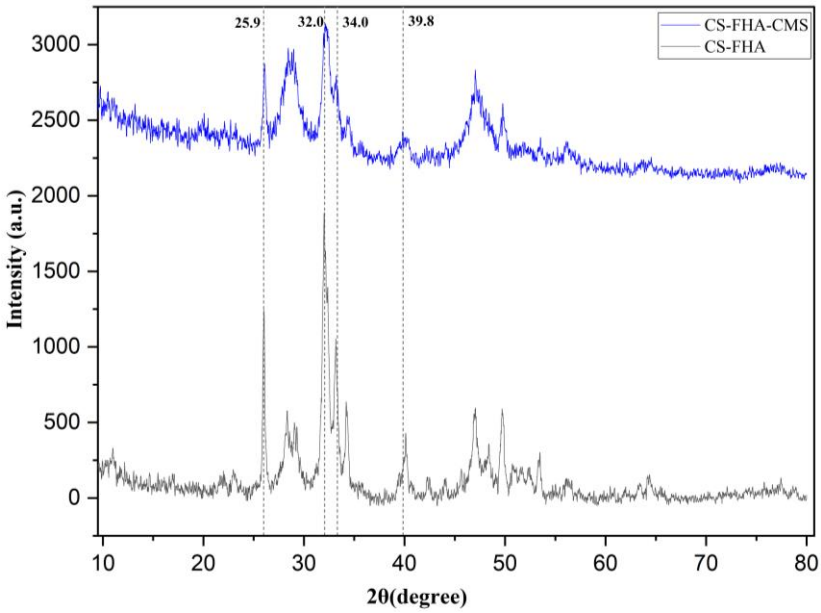

Figure 2: XRD of CS–FHA and CS–FHA–CMS nanocomposites.

XRD analysis was performed to investigate the crystallographic structure of the synthesised nanocomposites (Fig. 2). The diffraction pattern of CS–FHA exhibits characteristic peaks at 2θ ≈ 25.9°, 32.0°, 34.0°, and 39.8°, corresponding to the typical reflections of fluorine-substituted hydroxyapatite and confirming the presence of the apatite crystalline phase [16, 17]. These reflections can be indexed to the (002), (211), (300), and (310) planes of the apatite structure. A broad hump between 20° and 30° is also observed, which is attributed to the amorphous nature of chitosan overlapping with the apatite reflections [3, 18]. In the CS–FHA–CMS nanocomposite, the principal FHA peaks are retained, indicating that the incorporation of *CMS* extract does not disrupt the apatite crystal structure. However, a slight decrease in peak intensity with minor peak broadening is observed compared with CS–FHA, which may be attributed to the presence of amorphous organic constituents from the plant extract within the composite matrix [19].

3.3 SEM morphological analysis

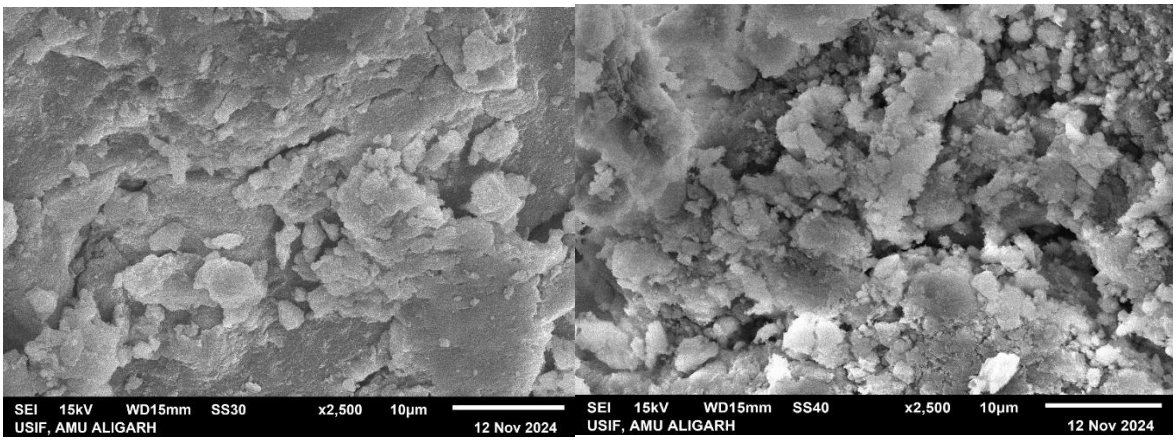

Figure 3: SEM micrographs of CS–FHA and CS–FHA–CMS nanocomposites.

SEM micrographs revealed a rough and porous surface morphology with interconnected features across the ternary nanocomposite (Fig. 3). The observed micro- and nanoscale surface irregularities increase surface area, which is favourable for cell attachment and nutrient transport [20]. Such porous architectures resemble natural bone structure and are widely reported to promote osteoblast adhesion and proliferation [21]. The morphology also suggests effective interaction among chitosan, FHA, and CMS.

3.4 In-vitro bioactivity in simulated body fluid

In vitro bioactivity was evaluated by immersion of the nanocomposite in simulated body fluid. SEM observations after immersion revealed the formation of apatite-like mineral layers on the surface of the composite (Fig. 4), indicating the composite's bioactive nature [22]. Apatite nucleation signifies a favourable interaction between the composite surface and physiological ions. The presence of surface phosphate and hydroxyl groups, along with polyphenolic constituents, likely facilitates calcium–phosphate ion exchange and promotes biomineralization [21].

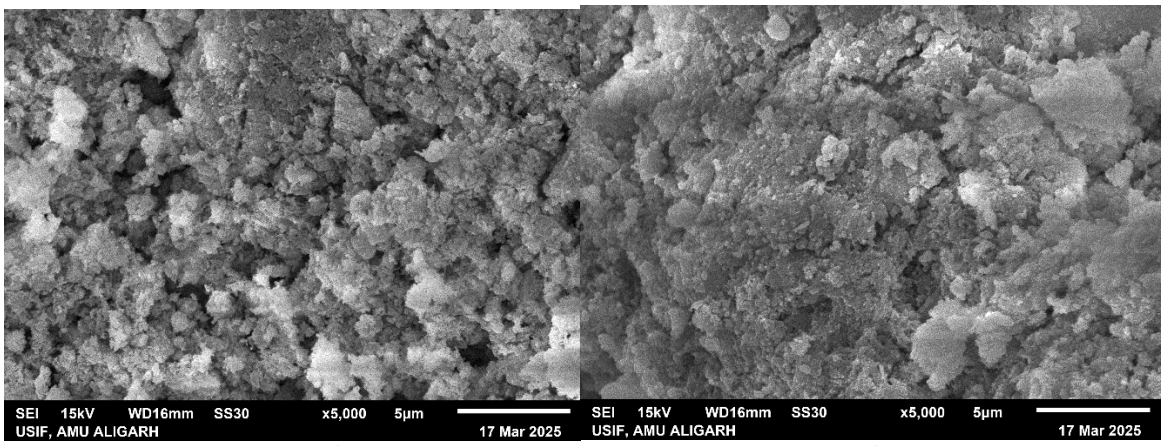

Figure 4: SEM Micrographs of CS-FHA and CS–FHA–CMS Composites at 15 days of biomineralisation studies.

3.5 Cytocompatibility assessment (MTT Assay)

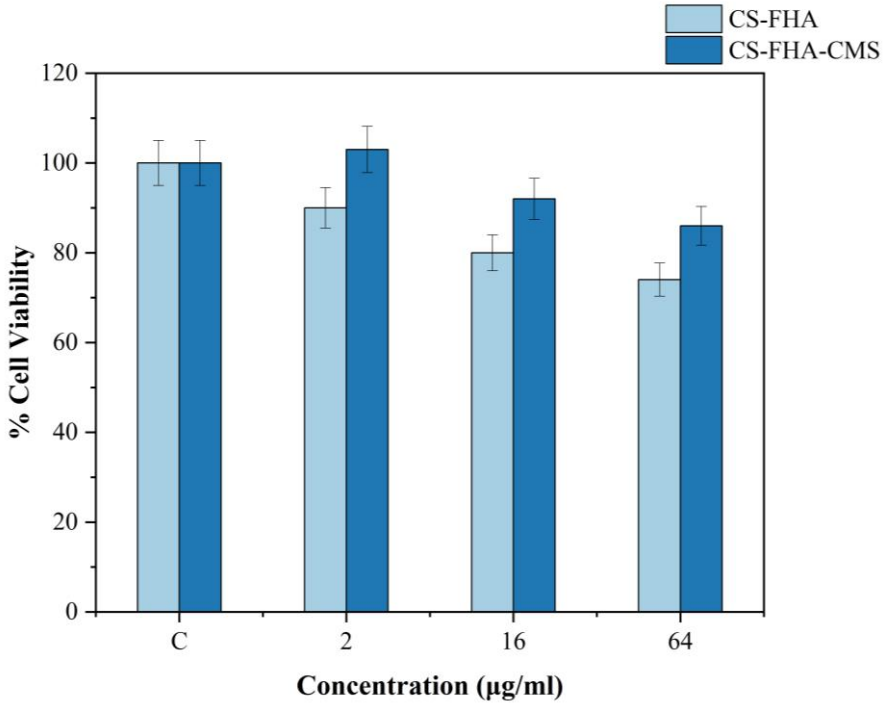

Figure 5: Cell viability of CS-FHA and CS–FHA–CMS at different concentrations.

Cell viability of the nanocomposites was assessed at concentrations of 2–64 µg mL^{-1} (Fig. 5). Both CS–FHA and CS–FHA–CMS maintained high viability relative to the control (~100%), indicating acceptable cytocompatibility. At 2 µg mL^{-1}, the ternary composite showed slightly higher viability (~103%) compared with CS–FHA (~90%), suggesting that bioactive constituents from CMS may modestly influence cellular metabolic activity [23, 24]. With increasing concentration, a gradual reduction in viability was observed for both materials; however, CS–FHA–CMS consistently retained

higher viability than the binary system. This behaviour may be associated with the combined effects of chitosan and fluorohydroxyapatite, which provide a biocompatible surface, while phytochemicals from CMS may contribute mild cytoprotective effects [25]. Overall, the results suggest that the ternary nanocomposite exhibits favourable cytocompatibility relevant to Bone Tissue Engineering applications.

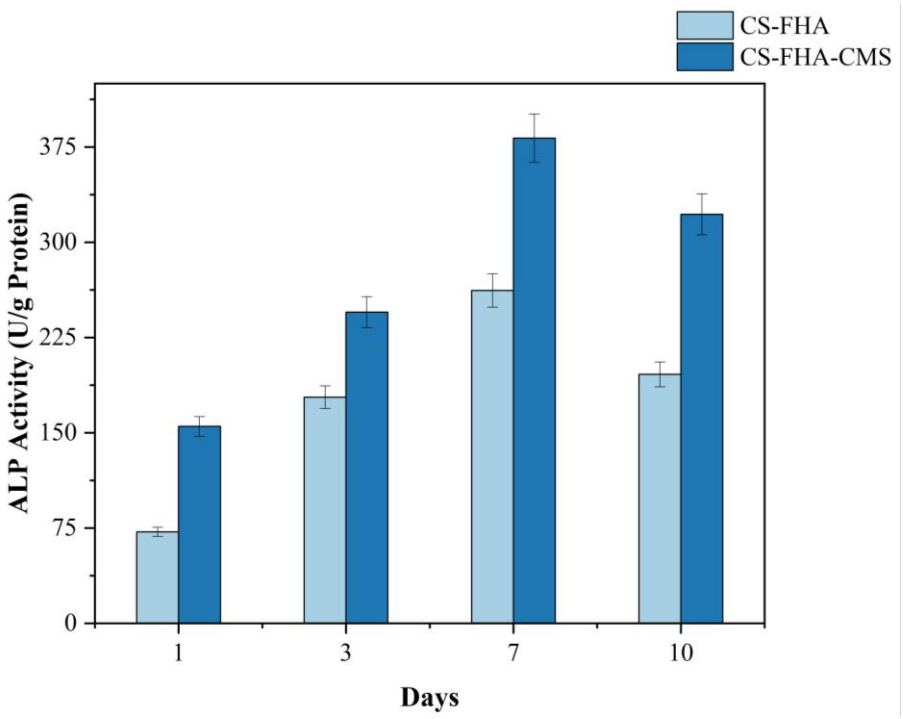

Figure 6: Time-dependent ALP activity of MG-63 cells.

ALP activity was monitored from day 1 to day 10 to assess the osteogenic response of the nanocomposites (Fig. 6). Both CS–FHA and CS–FHA–CMS exhibited a progressive increase in ALP activity from day 1 to day 7, followed by a slight decline at day 10. Notably, the ternary CS–FHA–CMS system consistently exhibited higher ALP levels than the binary composite. This trend suggests that the incorporation of CMS may enhance the early osteogenic response [12, 26]. The observed increase in ALP activity up to day 7 may be attributed to favourable cell–material interactions provided by CS and FHA, which offer a bioactive surface that can support osteoblastic differentiation. The subsequent reduction at day 10 may indicate progression toward later stages of matrix maturation [27]. Collectively, these findings suggest that the ternary nanocomposite elicits a relatively stronger ALP response relevant to bone tissue engineering applications.

4. Conclusions

A CS-FHA-CMS ternary nanocomposite was successfully developed and evaluated through physicochemical characterisation and preliminary biological validation. FTIR and XRD analyses confirmed retention of the FHA phase and presence of biologically relevant functional groups, while SEM revealed a rough and porous morphology favourable for bone tissue integration. In vitro bioactivity in simulated body fluid demonstrated apatite formation, indicating osteoconductive behaviour. Short-term cytocompatibility assessed by MTT assay confirmed the non-cytotoxic nature of the composite. The combined effects of fluorine doping, CS matrix support, and polyphenol-rich *CMS* suggest that the developed ternary nanocomposite possesses promising attributes for bone tissue engineering applications. Further studies may focus on advanced biological evaluation and optimisation of the composite system.

Acknowledgements

The authors acknowledge the Department of Chemistry, Aligarh Muslim University, Aligarh, India, for providing laboratory facilities for this research.

Authors' contributions

The author read and approved the final manuscript.

Conflicts of interest

The author declares no conflict of interest.

Funding

This research received no external funding.

Data availability

No new data were created.

References

[1] A.S. Safavi et al., Fabrication and characterization of chitosan-poly (3-hydroxybutyrate) scaffold as a novel 3D-printed platform for bone tissue engineering application, *Mater. Chem. Phys.* (2026) 132248.
[2] M. Kaveri et al., Synthesis of Limonia acidissima gum-based biopolymer/samarium substituted hydroxyapatite biocomposite for bone tissue engineering applications, *Int. J. Biol. Macromol.* (2026) 151148.
[3] F. Mushahid et al., Development of biomimetic nanocomposite scaffolds for bone tissue engineering applications using chitosan,

fluorohydroxyapatite, and Moringa oleifera leaf extract, *ChemistrySelect* (2026).
[4] L. Wang et al., Polyetheretherketone/nano-fluorohydroxyapatite composite with antimicrobial activity and osseointegration properties, *Biomaterials* 35 (2014) 6758–6775.
[5] S.D. Purohit et al., Chitosan-based electrospun fibers for bone-tissue engineering: Recent research advancements, *Int. J. Biol. Macromol*. (2024).
[6] J. Borges-Vilches et al., Multifunctional chitosan scaffold platforms loaded with natural polyphenolic extracts for wound dressing applications, *Biomacromolecules* **24** (2023) 4278–4293.
[7] G. Yu et al., Bone tissue engineering via nanocomposite scaffolds loaded with Camellia sinensis extract and bone marrow mesenchymal stromal cells, *J. Med. Biol. Eng*. **45** (2025).
[8] T. Fatima et al., Combinatorial approach to fabricate silica doped polyvinyl alcohol/ hydroxyapatite/ carrageenan nanocomposite for bone regeneration applications, *Polym. Adv. Technol*. (2023).
[9] I. Pawlaczyk-Graja et al., Effect of various extraction methods on the structure of polyphenolic-polysaccharide conjugates from Fragaria vesca L. leaf, *Int. J. Biol. Macromol*. **130** (2019) 664–674.
[10] T. Fatima et al., Hydroxyapatite/chondroitin sulphate nanocomposite infused with black seed oil for bone tissue applications: Physicochemical characterizations and in vitro screening, *ChemistrySelect* (2024).
[11] J. Chen et al., Multifunctional chitosan-hydroxyapatite-polyphenol nanoparticles from 3D printed bone scaffolds: Controlled release and therapeutic properties, *Eur. Polym. J*. (2025) 113738.
[12] Q. Wang et al., Engineering polyphenol-based osteogenic system for bone and cartilage repair: Transplantation, tissue engineering, and organoid, *J. Adv. Res*. (2025).
[13] R. Lopes et al., Formulation and characterization of chitosan-based mixed-matrix scaffold for tissue engineering, *Macromol*. **4** (2024) 253–268.
[14] A. Amri et al., Facile fabrication of Cu/Al LDH-Camellia sinensis extract composite for enhanced visible-light-driven photocatalytic degradation of ceftriaxone with mechanistic insights, *Next Mater*. (2026) 101981.
[15] R. Jolly et al., Zizyphus mauritiana seed extract: Paving the way for next-generation bone constructs with nano-fluorohydroxyapatite/carboxymethyl chitosan nanocomposite scaffold, *Int. J. Biol. Macromol*. (2024).
[16] Z. Jafari et al., Surface modification of AZ31 Mg alloy by diopside/fluorohydroxyapatite/graphene oxide nanocomposite coating: Corrosion and bioactivity evaluations, *J. Alloys Compd*. (2024).
[17] T.J. Yin et al., Characterization of porous fluorohydroxyapatite bone-scaffolds fabricated using freeze casting, *J. Mech. Behav. Biomed. Mater*. **122** (2021) 104717.
[18] F. Tondnevis et al., Using chitosan besides nano hydroxyapatite and fluorohydroxyapatite boost dental pulp stem cell proliferation, *J. Biomimetics Biomater. Biomed. Eng*. **42** (2019) 39–47.
[19] D. Gopi et al., A novel green template assisted synthesis of hydroxyapatite nanorods and their spectral characterization, *Spectrochim. Acta Part A Mol. Biomol. Spectrosc*. **107** (2013) 196–202.
[20] S. Shendage et al., Nanohydroxyapatite and its composite scaffold for bone tissue engineering application: A systematic review, *J. Mater. Sci. Mater. Med*. **36** (2025).
[21] X. Ren et al., Novel synthesis approach for natural tea polyphenol-integrated hydroxyapatite, *Pharmaceuticals* **17** (2024) 251.
[22] M. Shakir et al., Fabrication and characterization of nanoengineered biocompatible n-HA/chitosan-tamarind seed polysaccharide: Bio-inspired nanocomposites for bone tissue engineering, *Int. J. Biol. Macromol*. **111** (2018) 923–933.
[23] M. Sánchez et al., The pharmacological activity of Camellia sinensis (L.) Kuntze on metabolic and endocrine disorders: A systematic review, *Biomolecules* **10** (2020) 603.
[24] N. Singh et al., Phytochemistry and anticancer therapeutics of Camellia sinensis (Green tea), *Pharmacol. Res. Mod. Chin. Med*. (2024) 100484.
[25] R. Chelliah et al., Camellia sinensis (Green tea): Unveiling the anti-inflammatory and antioxidant symphony in inflammatory bowel diseases, harmonizing with molecular pathways of therapeutic, *Pharmacol. Res. Nat. Prod*. (2025) 100435.
[26] C. Kulkarni et al., Evaluation of antiosteoporosis effects of Camellia sinensis (tea), its extracts, and major compounds, in: Tea in Health and Disease Prevention, *Elsevier* (2025).
[27] V. Chawla et al., ALP-mimetic cyclic peptide nanotubes: A multifunctional strategy for osteogenesis and bone regeneration, *Biomacromolecules* (2025).